Sedimentology (1994) **41**, 409–421

Diagenetically altered sabkha-type Pleistocene dolomite from the Arabian Gulf

HENRY S. CHAFETZ *and* PATRICK F. RUSH*

Department of Geosciences, University of Houston, Houston, TX 77204-5503, USA

ABSTRACT

Diagenetically altered Pleistocene dolomite occurs in the shallow subsurface of the Arabian Gulf, offshore of Al Jubayl, Saudi Arabia. This dolomite accumulated in relatively shallow marine to sabkha depositional environments. In contrast with the thin extent of most other Quaternary sabkha and sabkha-related dolomite deposits, these deposits comprise a thick (>56 m) accumulation. Additionally, this Pleistocene dolomite displays a high degree of ordering and has a more nearly ideal stoichiometric composition than the dolomite from the depositionally and diagenetically analogous Abu Dhabi sabkha complex. The Pleistocene dolomite also has lower $\delta^{13}C$ and $\delta^{18}O$ values than the modern Abu Dhabi sabkha dolomite, and higher values than those commonly reported for analogous dolomite from the ancient rock record. The low $\delta^{18}O$ values, in conjunction with the geological setting, indicate that the diagenetic waters were meteoric or mixed meteoric and marine in composition. Thus, the degree of ordering, stoichiometric and stable isotopic values indicate that this dolomite has undergone diagenetic alteration relative to its presumed Holocene precursor.

INTRODUCTION

The lower part of an extensive suite of Quaternary sediment and rock samples from under the nearshore part of the Arabian Gulf, offshore of Al Jubayl, Saudi Arabia, is the subject of this investigation (Fig. 1). Although modern sediments within the Arabian Gulf have been intensively studied during the last 35 years (e.g. Emery, 1956; Houbolt, 1957; Wells & Illing, 1964; Illing *et al.*, 1965; Butler, 1969; Fuchtbauer, 1969; Kendall & Skipwith, 1969a,b; Purser, 1973a, 1979; Picha, 1978; McKenzie *et al.*, 1980; McKenzie, 1981; Patterson & Kinsman, 1982; Ellis & Milliman, 1985; Khalaf *et al.*, 1984, 1987; Al-Ghadban, 1990), especially since this area was recognized as a site of extensive carbonate deposition, there have been only a small number of investigations concerned with the Quaternary sediments below the top few metres of the modern accumulations. A suite of intercalated carbonate and siliciclastic sediments and rocks recovered from a line of boreholes was analysed during this investigation. Previous analyses (Chafetz *et al.*, 1988), as well as new data, show that the overall accumulation can be readily divided into three diagenetic facies: a lowermost dolomitic facies, a middle low-magnesian calcitic facies and an uppermost aragonitic facies (Fig. 2). The dolomite is Pleistocene and possibly older in age. Evaporite and siliciclastic deposits, as well as a trace admixture of aragonitic and calcitic constituents, occur within the dolomite. These strata are overlain by an accumulation composed of subequal amounts of low-magnesian calcitic and siliciclastic deposits, which, in turn, are overlain by aragonitic sediments with a relatively minor admixture of siliciclastics. The dolomite is the prime subject of this investigation.

SAMPLES

The suite of samples was picked from 31 essentially equally spaced borings, which were drilled as part of a foundation engineering study for a trestle and sea dock, in the Arabian Gulf, offshore from Al Jubayl, Saudi Arabia. The line of borings extends 9·4 km gulfward, with the shoreward end in less than 1 m of water and the gulfward end in 23·4 m of water. The borings penetrated between 15·2 and 61·6 m of

*Present address: Reservoirs, Inc., 1151-C Brittmore Road, Houston, TX 77043, USA.

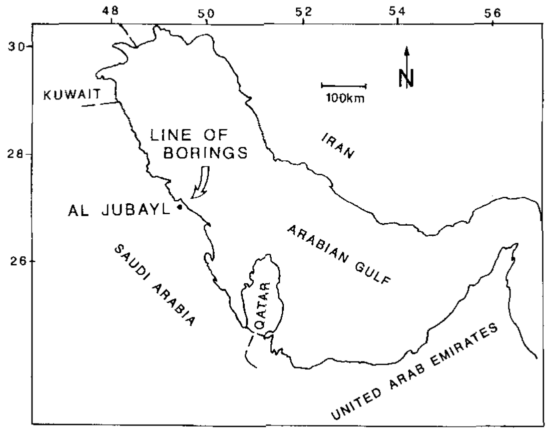

Fig. 1. Map showing the location of the line of borings which extend approximately 10 km seaward, perpendicular to the shoreline, offshore of Al Jubayl, Saudi Arabia, within the Arabian Gulf.

sediment, and average 27 m long (Fig. 2). Samples from the borings were collected by the foundation engineers approximately every 2 m and, in addition, at all major lithological changes. Approximately 450 individual samples, ranging from unconsolidated to well lithified (mostly semilithified), were collected; 164 samples came from the dolomitized part of the accumulation. All samples were stored in wide mouth jars and forwarded to Houston for analyses. Thus, for many of the samples, sedimentary structures and textural relationships were not preserved nor were any water samples collected. Additionally, 23·8 m of lithified core was collected and analysed. This study is based entirely on analyses of the individual samples and core; the authors were not present at the time of sampling.

METHODS

Standard binocular, petrographic, cathodoluminescent, SEM and XRD techniques were employed for sample analyses. Freshly broken samples as well as those immersed overnight in dilute H_2O_2 were viewed using an SEM. Predominantly, whole rock samples of the dolomite were analysed as well as some samples of individual allochems (i.e. red algae, echinoids) for their stable isotopic composition. Some individual samples within a jar were composed of

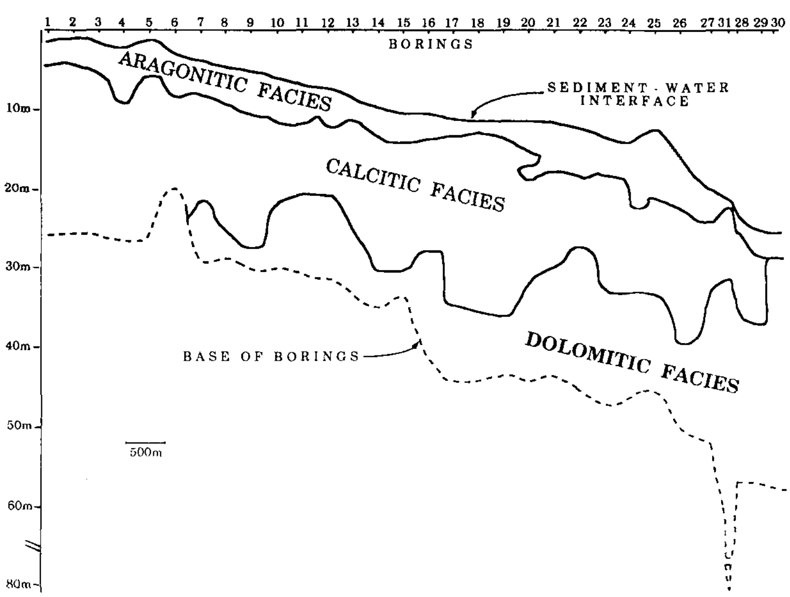

Fig. 2. Schematic cross section showing the relative location of borings, depth from sea level to the sediment–water interface along the line of borings, depth of borings within the sediments, and distribution of the three diagenetic facies (dolomitic facies at base, low-magnesian calcitic facies in the middle and the aragonitic facies occupying the topmost part of the cross section). Vertical exaggeration × 100.

more than one lithological type of dolomite and, therefore, sometimes analyses were conducted on different varieties of dolomite from a single jar (e.g. two analyses were performed on different portions of the sample collected from boring 10 at a depth of 21·2 m; see Table 2). The isotopic results reported for the dolomite come only from samples that microscopic and XRD analyses confirmed to be essentially composed of 100% dolomite. A CaF_2 standard was added to each sample prior to XRD analyses. The calcium content was determined by the 2θ displacement of the (104) peak (Goldsmith *et al.*, 1961) and the degree of ordering in the dolomite was determined by dividing the intensity of the ordering of line (015) by the intensity of the (110) line in the XRD patterns (Goldsmith & Graf, 1958). (The authors are aware that there are numerous limitations in determining composition and degree of ordering by XRD methods; Land, 1985, 1986.) ^{14}C analyses were performed on 11 samples, three from the dolomitic facies, by commercial laboratories. Oxygen and carbon isotopic compositions were determined using a Finnigan-MAT Delta E mass spectrometer. Carbonate samples were reacted with H_3PO_4 at 50°C (modified method of McCrea, 1950). Replicate analyses showed that, in our laboratory, the $\delta^{18}O$ values for Al Jubayl dolomite digested at 50°C are 0·95‰ lower than those digested at 25°C. The dolomite values reported have not been corrected to correspond with values obtained at 25°C nor have they been corrected for fractionation which occurs during digestion relative to calcite (Sharma & Clayton, 1965; Land, 1980, 1985). Carbon and oxygen isotopic values have been corrected for ^{17}O abundances and all isotopic data pertaining to sediment and rock are reported relative to PDB (Craig, 1953).

PETROGRAPHY

Overview

Recent paralic sediments accumulating along the southern Arabian Gulf, adjacent to the United Arab Emirates, dominantly comprise carbonates, whereas sediments adjacent to Kuwait are dominated by siliciclastics. The area from which the samples were obtained is located between the loci of dominantly carbonate deposits to the south-east and predominantly siliciclastic deposits to the north-west and, consequently, the section investigated consists of a subequal mixture of carbonates and siliciclastics. These deposits display a complex interfingering of a wide variety of lithological types.

The sediments and rocks that comprise this vertically distributed suite of samples are compositionally similar to sediments presently being deposited in the Arabian Gulf (Clarke & Keij, 1973; Purser, 1973b; Wagner & van der Togt, 1973). Molluscs, echinoderms, corals, red algae, pellets, ooids and intraclasts comprise the majority of the allochems (McIntosh, 1983; Chafetz *et al.*, 1988). Siliciclastic material ranges in abundance from trace amounts to the most abundant constituent. The siliciclastic grains are dominantly quartz, although a variety of feldspars, rock types and heavy minerals are commonly present (Pierce, 1990).

In addition to the complex depositional pattern, the sediments have been affected by a variety of diagenetic processes, including cementation, stabilization of high-magnesian to low-magnesian calcite, dissolution, dolomitization and precipitation of evaporites. Due to the pervasive nature of some of the diagenetic processes, the total accumulation has been divided into three diagenetic facies: a dolomitic facies, a low-magnesian calcitic facies, and an aragonitic facies (Fig. 2). The dolomitic facies is always lowermost, the low-magnesian calcitic facies occupies the middle position and the aragonitic material occurs at the surface of the deposit.

The dolomitic facies is primarily composed of aphanocrystalline dolomite with intercalated layers and individual crystals of gypsum and anhydrite. A trace admixture of non-dolomitized calcite and aragonite also occurs within this facies. The low-magnesian calcitic facies ranges from 5 to 23 m in thickness (Fig. 2). This facies is composed of subequal amounts of carbonate and siliciclastic deposits. The carbonate sediment and rock are predominantly composed of low-magnesian calcite; however, isolated packets of non-altered aragonitic and high-magnesian calcitic material occur within this diagenetic facies. In the altered sediment, the formerly aragonitic constituents are represented by biomouldic porosity whereas formerly high-magnesian allochems have stabilized to low-magnesian calcite and have commonly been thoroughly micritized. Thin isopachous rims of non-luminescent low-magnesian calcite cement partially fill biomouldic pores and interparticle porosity (Chafetz *et al.*, 1988, fig. 4). The aragonitic facies comprises approximately the topmost 5 m of the sediment package and is composed of essentially unaltered shallow marine allochems. The sediment has only undergone diagenesis in the shallow marine realm, e.g. cementation by isopachous fibrous aragonite.

^{14}C age dates

Holocene age dates have been obtained from unaltered aragonitic skeletal material from the aragonitic diagenetic facies. In contrast, Pleistocene age dates have been obtained from whole rock material of altered low-magnesian calcitic material as well as the dolomitic material. Thus ^{14}C age dates and sedimentological and diagenetic analyses (Chafetz *et al.*, 1988) indicate that the dolomitic strata are Pleistocene whereas the aragonitic deposits are Holocene in age.

Dolomite

Sedimentology

Dolomite comprises the lowermost portion of most of the 31 borings (Fig. 2). Despite the pervasive diagenetic overprint on the dolomitized deposits, most of the same suite of constituents comprising the overlying calcitic and aragonitic deposits can be recognized within the dolomite. In general, the dolomitized deposits are semilithified and, thus, sedimentary structures are better preserved than in the calcitic or aragonitic portion of the overall accumulation. In contrast to the overlying deposits, the dolomite contains evaporites and only a relatively sparse admixture of siliciclastic grains whereas no evaporites exist within the calcitic and aragonitic strata, and siliciclastics are relatively abundant in the calcitic deposits.

A modest spectrum of sedimentary structures is evident within the semilithified dolomite samples. An association is evident between the type of sedimentary structure(s) observed and the presence or absence of particular constituents. Bioturbated samples commonly contain skeletal material, either whole and/or abraded shells (Fig. 3A). Within the bioturbated samples, traction transport sedimentary structures were not recognized. These samples are interpreted as subtidal in origin and comprise approximately one-third of the samples which could be classified according to depositional environment. A different suite of samples displayed laminated dolomite, on a millimetre to centimetre scale, mixed bedding (clay-rich laminae interlaminated with sandy laminae), the presence of rounded as well as angular intraclasts, and only a minor amount of bioturbation. This dolomite is interpreted as representative of deposition in an intertidal environment (Fig. 3B, C). Intertidal deposits make up approximately one-half of the samples classified. A few samples comprise finely laminated deposits with intraclasts, desiccation-cracked laminae, and evaporites, gypsum and/or anhydrite. The evaporites occur as individual crystals (commonly discoidal in morphology) and splays of crystals, as well as nodules and solid 'horizons' of chickenwire evaporites (Fig. 3D). There is a paucity of skeletal debris within these finely laminated deposits. This finely laminated dolomite with its associated evaporites has been interpreted as supratidal in origin. A depositional environment could not be determined for approximately one-sixth of the dolomite samples. Thus, by use of the combination of sedimentary structures and sediment composition, most of the samples were recognized as having accumulated in subtidal, intertidal or supratidal depositional environments.

Table 1. Summary statistics for 122 dolomite samples.

	Mean	n	SD	Range
Ca content (mol%)	51·40	101	1·22	49·6–56·6
Ordering	0.70	97	0·15	0·41–1·28
$\delta^{13}C$ (‰)	1·42	122	1·54	4.41 to −4·58
$\delta^{18}O$ (‰)	0·61	122	1·04	4·11 to −2·50

For comparative purposes with analyses conducted at other laboratories, our laboratory replicate runs indicate that had the dolomite been analysed at 25°C, rather than at 50°C, the $\delta^{18}O$ values would have been approximately 0·95‰ higher than those reported. Sample by sample analyses are provided in Table 2.

Crystal chemistry

The deposit is dominantly composed of aphanocrystalline to very fine crystalline (2–15 μm) dolomite. Most of the dolomite is fairly uniform in size; however, some samples show a wide range of crystal size (Fig. 4). Most of the dolomite is anhedral to subhedral and the crystals have a somewhat rounded appearance; euhedral dolomite crystals rarely occur (Fig. 5). The crystal chemistry of the dolomite, as determined by XRD and stable isotopic analyses, is summarized in Table 1 and listed for individual samples in Table 2. No differences, with one exception, were noted in the morphology, chemical composition, degree of ordering, etc., of the dolomite crystals from the different depositional environments.

None of the four variables (Ca content, degree of ordering, $\delta^{13}C$ and $\delta^{18}O$) displayed any consistent

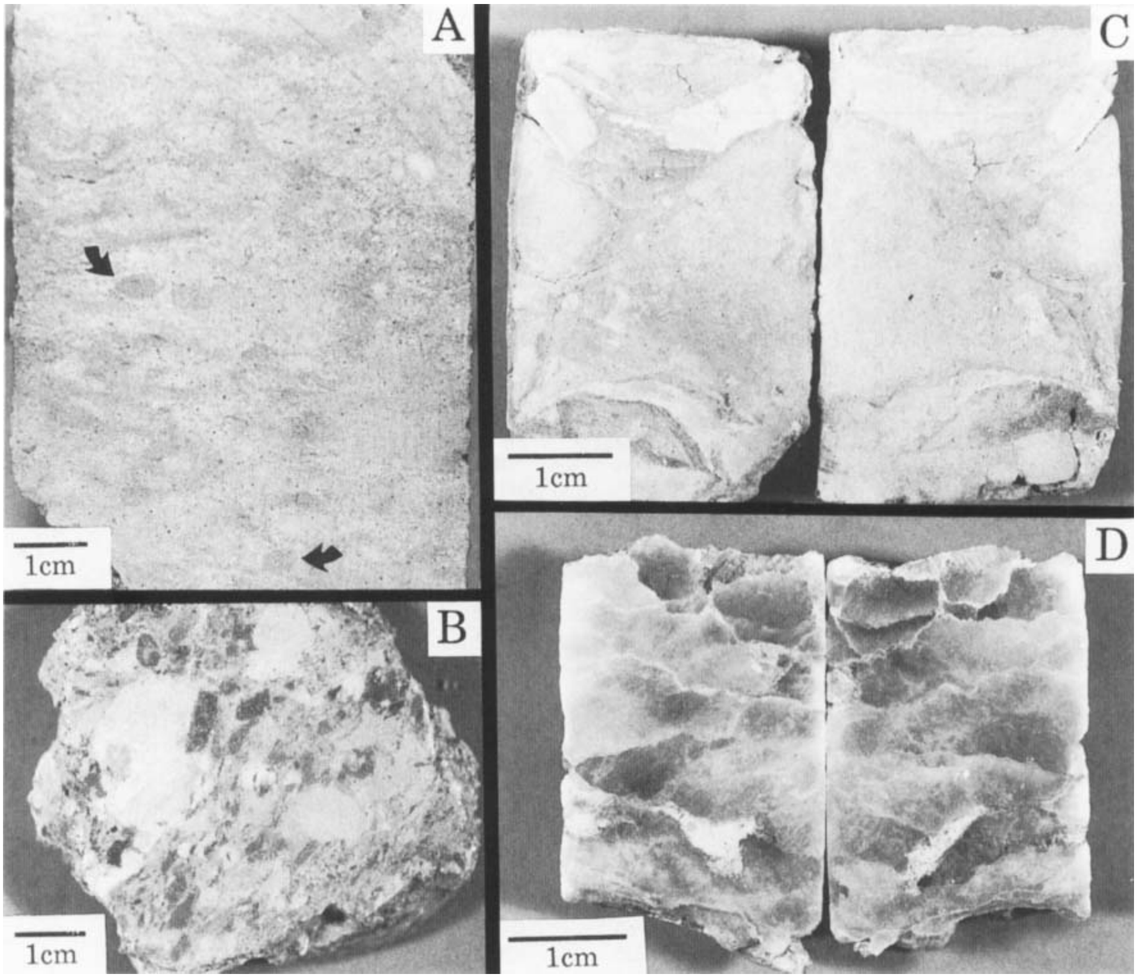

Fig. 3. A representative suite of the different lithological types recognized within the dolomitic accumulation: (A) thoroughly bioturbated (arrows) dolomitized biomicrite; (B) a semilithified deposit composed of a varied suite of rounded and angular intraclasts; (C) the angular intraclasts present near the top of this sample display finely laminated internal structure and probably originated as desiccation-cracked laminae in the supratidal environment; (D) solid core of gypsum displaying chickenwire structure.

trend either down the borings or laterally along the accumulation. The means, standard deviations, etc., of the four variables were computed for the samples comprising the subtidal, intertidal and supratidal depositional facies. In general, the values for the various attributes are similar between the deposits from the different environments. The only readily apparent difference is between the $\delta^{13}C$ values of the dolomite from the supratidal depositional environment and those from the intertidal and subtidal environments. However, only four samples from the supratidal environment were confidently recognized and analysed, a very small sample set. Nevertheless, two-tailed t-tests indicated that statistically there is less than 0·05 and 0·10 probability that carbon from the supratidal and intertidal environments and from the supratidal and subtidal environments, respectively, are part of the same populations.

Bivariant plots of the four variables display considerable scatter (Fig. 6). However, trends do exist between some of the variables. Even though the bivariant plots display considerable scatter, and thus

Table 2. Data on individual samples.

Bore	Depth (m)	$\delta^{13}C$ (‰)	$\delta^{18}O$ (‰)	Ca content (%)	Ordering	Depositional environment*
7	26·5	1·39	−0·35	49·6	0·5	2
7	26·5	1·29	−0·67	49·6	0·5	2
8	24·0	1·90	0·61	52 7	0·6	4
8	26·2	−2.77	2·31	49·9	0·9	3
9	24·8	−0·84	−0·40	50·5	0·9	3
10	21·2	2·08	0·65			3
10	21·2	2·02	0·98	50·5	0·6	3
10	24·7	2·72	0·91	51·4	0·8	3
10	24·9	1·23	0·20	50·8	0·5	3
10	27·8	1·67	0·80	50·8	0·7	2
11	19·5	2·87	0·67	53·3	0·8	4
11	22·8	2·31	−1·43			4
11	25·1	2·64	−0·06	49·9	1·0	2
11	25·3	1·29	−0·34	51·4	0·8	2
12	20·1	3·68	0·97	51·4	0·5	3
12	20·1	3·67	0·94	51·4	0·5	3
12	23·0	1·86	0·93	50·8	0·5	2
12	23·0	−1·02	0·51	52·0	0·7	2
12	25·3	1·84	0·16	51·4	0·7	3
12	28·2	1·49	−0·74	52·4	1·0	2
12	29·6	1·21	−0·24	51·4	0·6	2
13	24·1	1·37	0·36			4
13	24·1	1·76	1·20	51·4	0·6	4
13	25·8	3·62	1·10	51·1	0·7	2
13	29·2	1·02	−0·04	51·7	0·7	1
13	32·1	0·76	−0·07	53·0	0·7	2
14	29·1	2·64	1·45			2
14	29·1	1·53	1·54	49·6	0·7	2
14	29·1	2·12	2·51	49·6	0·7	2
14	29·3	2·56	1·91	54·2	0·7	2
14	32·3	2·35	0·69	51·1	0·6	2
14	32·3	0·04	1·50	52·0	0·6	2
14	32·3	−0·10	−0·69	52·0	0·6	2
14	32·5	1·86	1·20	52·7	0·5	4
16	28·3	1·33	3·38	53·3	0·5	3
16	34·2	1·52	0·12	51·7	0·7	3
16	39·4	3·25	0·67	51·1	0·7	4
17	35·0	3·27	1·87	50·8	0·6	4
17	38·5	2·46	1·32	53·0	0·6	2
17	38·5	1·25	1·92	51·7	0·8	2
17	38·8	1·54	1·86	52·0	0·8	2
17	41·4	3·57	2·46	50·8	0·7	2
18	33·1	3·36	0·04	51·0	0·7	2
18	41·6	1·81	0·20	51·4	0·9	2
19	28·4	1·19	−1·07			3
19	34·5	1·56	0·65	49·6	0·7	2
19	37·7	−2.15	−0·07	51·4	0·8	4
19	40·6	1·14	0·47	51·4	0·7	3
20	31·3	−0·37	0·68	51·8	0·8	3
20	33·9	1·70	0·60	50·5	0·7	4
20	34·3	1·04	0·11	52·0	0·8	2
21	27·9	0·77	−2·24	52·0	0·7	2
21	33·7	2·46	0·47	50·8	0·6	2
21	36·6	2·40	0·23	52·4	0·8	4
21	36·8	2·50	0·37	50·5	0·7	2

Table 2. *Continued.*

Bore	Depth (m)	$\delta^{13}C$ (‰)	$\delta^{18}O$ (‰)	Ca content (%)	Ordering	Depositional environment*
21	36·8	2·40	0·02	50·5	0·7	2
22	25·9	0·55	4·11	53·9	0·5	4
22	25·9	0·63	3·60	53·9	0·5	4
22	36·6	1·43	1·39	50·8	0·7	2
23	31·4	1·59	−0·13	52·7	0·6	2
23	31·5	1·56	0·15	49·9	0·5	3
23	31·5	1·74	−0·05	49·9	0·5	3
23	34·5	1·26	0·78	50·8	0·8	1
23	34·5	1·37	0·49	50·8	0·8	1
23	34·6	1·30	0·74	52·7	0·8	3
23	34·6	1·40	0·47	52·7	0·8	3
23	37·8	1·16	−0·69	51·4	0·7	3
23	37·8	1·24	−0·62	51·4	0·7	3
23	40·9	3·79	1·71	49·6	0·7	3
23	43·6	0·75	−0·08	53·3	0·7	2
23	43·6	3·93	1·51	53·3	0·7	2
24	29·1	1·71	2·41	56·6		3
24	31·7	−3·56	−2·50	50·8		3
24	31·7	−2·53	−0·60	50·8		3
24	33·0	−3·23	−0·89	51·4	0·8	2
24	33·0	−3·15	−0·68	51·4	0·8	2
24	40·3	3·18	1·23	49·9	0·4	2
24	43·2	1·21	−0·54	50·5	0·7	3
25	32·2	1·72	1·28	51·1	0·7	3
26	41·3	1·82	2·09			2
26	47·2	2·01	0·02	50·5	0·8	3
27	31·8	0·28	−0·11			2
27	31·8	0·11	−0·49			2
27	31·9	0·20	−0·80	50·8		2
27	37·9	3·14	0·96	53·3	0·6	3
27	37·9	3·06	0·75	52·4	0·7	3
27	43·9	0·26	0·60	51·1	0·7	2
27	47·5	1·68	1·31	50·8	0·6	3
27	48·8	2·29	0·66	49·9	0·6	3
27	49·1	1·58	0·74	50·8	0·6	3
28	36·9	2·29	1·81	51·4	0·5	4
28	47·2	0·76	0·26	52·4	0·7	3
28	47·2	1·53	−0·19			3
28	50·4	2·15	0·27			2
28	50·4	3·35	0·26			2
28	50·4	2·06	0·17			2
28	50·4	2·15	1·67			2
28	53·5	2·30	1·54	50·5	0·6	3
29	38·6	0·89	1·43	51·6	0·7	2
29	38·8	4·41	0·88	51·1	0·7	2
29	41·7	−0·16	1·00	51·4	1·3	2
29	44·9	1·60	0·98	50·8	0·8	3
29	50·8	2·17	0·54	52·4	0·8	4
29	53·7	2·66	0·53			4
29	53·7	2·08	−0·13			4
30	27·5	0·28	0·03			2
30	27·5	0·66	0·31			2
30	27·5	0·79	0·67	52·7	0·6	2
30	30·7	0·67	0·58	51·7	1·0	2
30	30·7	0·44	−0·15			2

Table 2. *Continued.*

Bore	Depth (m)	$\delta^{13}C$ (‰)	$\delta^{18}O$ (‰)	Ca content (%)	Ordering	Depositional environment*
30	35·2	3·02	0·46			2
30	35·2	3·04	0·63	51·7	0·6	2
30	44·5	1·66	0·74			4
30	54·4	−4·58	−1·05			1
31	29·7	1·92	1·08	50·5	1·0	2
31	32·3	−0·97	0·61	52·7	0·8	4
31	41·3	1·77	2·61	51·4	0·5	2
31	47·4	2·32	2·25	51·7	0·7	4
31	53·8	−0·02	0·20	49·6	1·0	2
31	60·5	1·69	0·47	53·6	1·0	3
31	69·3	1·31	0·60	49·6	0·7	3
31	80·8	1·60	1·19	50·2	0·4	3

*1, supratidal; 2, intertidal; 3, subtidal; 4, unknown. Various statistics computed from these data are given in Tables 1, 3 and 4.

have very low *r* values, the linear trends are statistically significant. The trends indicate that the crystals display a higher degree of ordering with lower $\delta^{13}C$ and $\delta^{18}O$ values (>99 and 97·5% confidence levels, respectively; Fig. 6A, B), and lower $\delta^{18}O$ values are also associated with lower Ca content (>99% confidence level; e.g. lower $\delta^{18}O$ values are present in the more nearly ideal stoichiometric dolomite; Fig. 6C). The best trend is exhibited by a bivariant plot of $\delta^{13}C$ and $\delta^{18}O$, which reveals a linear positive trend (>99% confidence level); lower $\delta^{13}C$ values are associated with lower $\delta^{18}O$ values (Fig. 6D). All four of the trends are reasonable and consistent with the concept of partial diagenetic alteration toward values common in the ancient rock record for sabkha dolomite.

DISCUSSION

Sedimentological evidence indicates that the dolomite deposit is Pleistocene and possibly older in age (Chafetz *et al.*, 1988). The sediment and rock comprising this deposit display evidence of subtidal, intertidal and supratidal depositional environments which probably accumulated as part of prograding sabkha complexes, similar to the modern Abu Dhabi

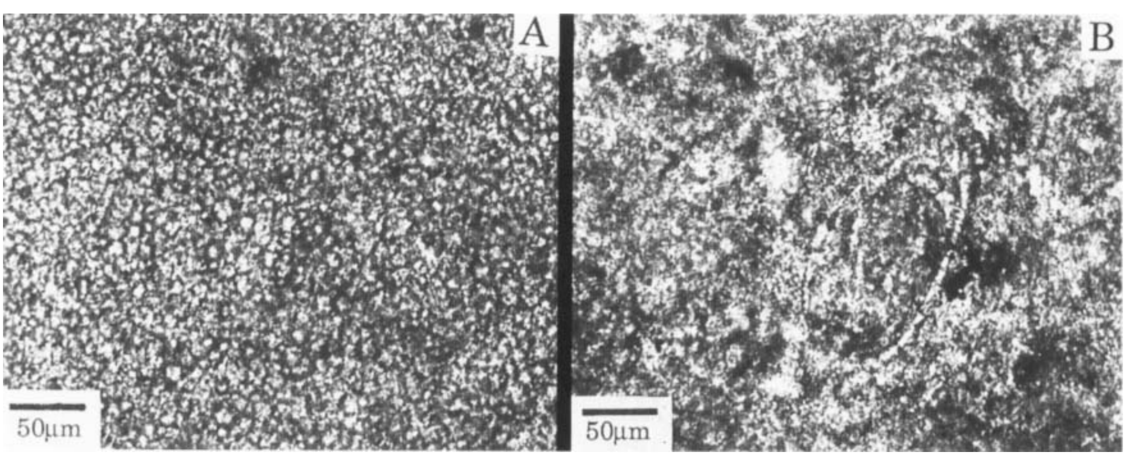

Fig. 4. Photomicrographs of dolomite composed of a homogeneous (A) and heterogeneous (B) distribution of crystal sizes. The fossil fragment shown in (B) is replaced by relatively coarse dolomite; some fossils, however, occur as thoroughly dolomicritized remains.

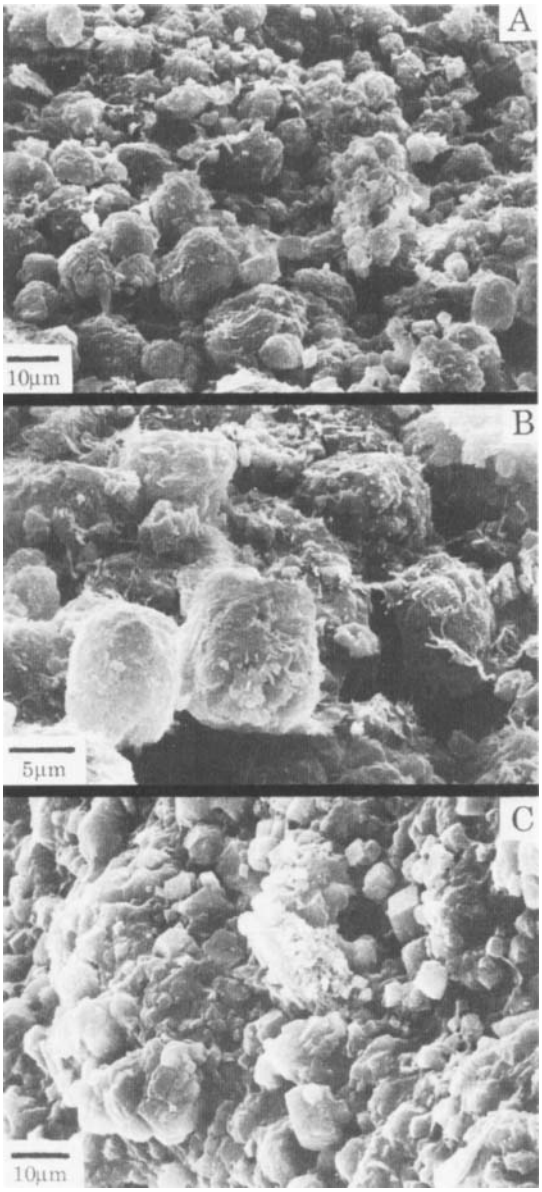

Fig. 5. (A, B) Two fields of view showing the predominantly anhedral to subhedral habits of the dolomite common throughout this accumulation. (C) An example of the relatively rare occurrence of euhedral dolomite.

sabkha complex. The sabkha-related depositional environments of this dolomite are not only indicated by its sedimentary structures, suite of sediment types and presence of evaporites within the deposits, but also by the near normal stoichiometry of the dolomite (Lumsden & Chimahusky, 1980). The sabkha depositional environment in which this dolomite formed, in conjunction with its relatively young age and geological setting, indicate that it was never deeply buried. The initial dolomitization must have occurred very early, while the sediments were in the near surface realm, analogous to the modern Abu Dhabi sabkha. This dolomite exceeds 56 m in total thickness; in contrast, modern sabkha dolomites tend to be thin accumulations (Machel & Mountjoy, 1986). Changes in the depositional environment displayed in the vertical succession within the borings suggest that the total dolomite deposit probably accumulated during more than one of the significant glacially induced sea level changes that occurred during the Pleistocene. Thus, the dolomite accumulation represents more than one period of progradation, progradation and regression, etc.; unfortunately, the nature of the samples provided to the investigators does not allow us to state with confidence how many cycles are represented in these borings. Work in progress, on other borings, indicates that the deepest borings may have penetrated at least two exposure surfaces. Thus, the Pleistocene Al Jubayl dolomite probably represents a number of major migrations of sabkha complexes due to the significant sea level changes which took place during the Pleistocene.

The whole rock mean $\delta^{18}O$ value obtained for the overlying aragonitic material (0·04‰, Table 3) is a reasonable approximation of the initial values for the now dolomitized carbonates prior to any diagenetic alteration. Modern Abu Dhabi sabkha sediments are diagenetically altered from aragonite to dolomite (McKenzie, 1981). The presence of fairly well preserved aragonitic fragments within the Pleistocene Al Jubayl dolomite indicates that this dolomite also was directly altered from aragonite to dolomite and not first altered to low magnesian calcite prior to dolomitization. However, the present dolomite has a much lower mean $\delta^{18}O$ value (0·61‰, Table 3) than expected for carbonates with (1) an initial value of the aragonitic facies (0·04‰; Land, 1980), (2) which formed in contact with the evaporative waters of a sabkha, or (3) in contact with marine waters. The lower $\delta^{18}O$ values relative to Holocene Arabian Gulf dolomite are presumably due to the influence of meteoric water on the dolomite. The low-magnesian calcitic facies displays many of the commonly recognized petrographic attributes of having been diagenetically altered under the influence of meteoric water in the phreatic zone (Chafetz *et al.*, 1988). In

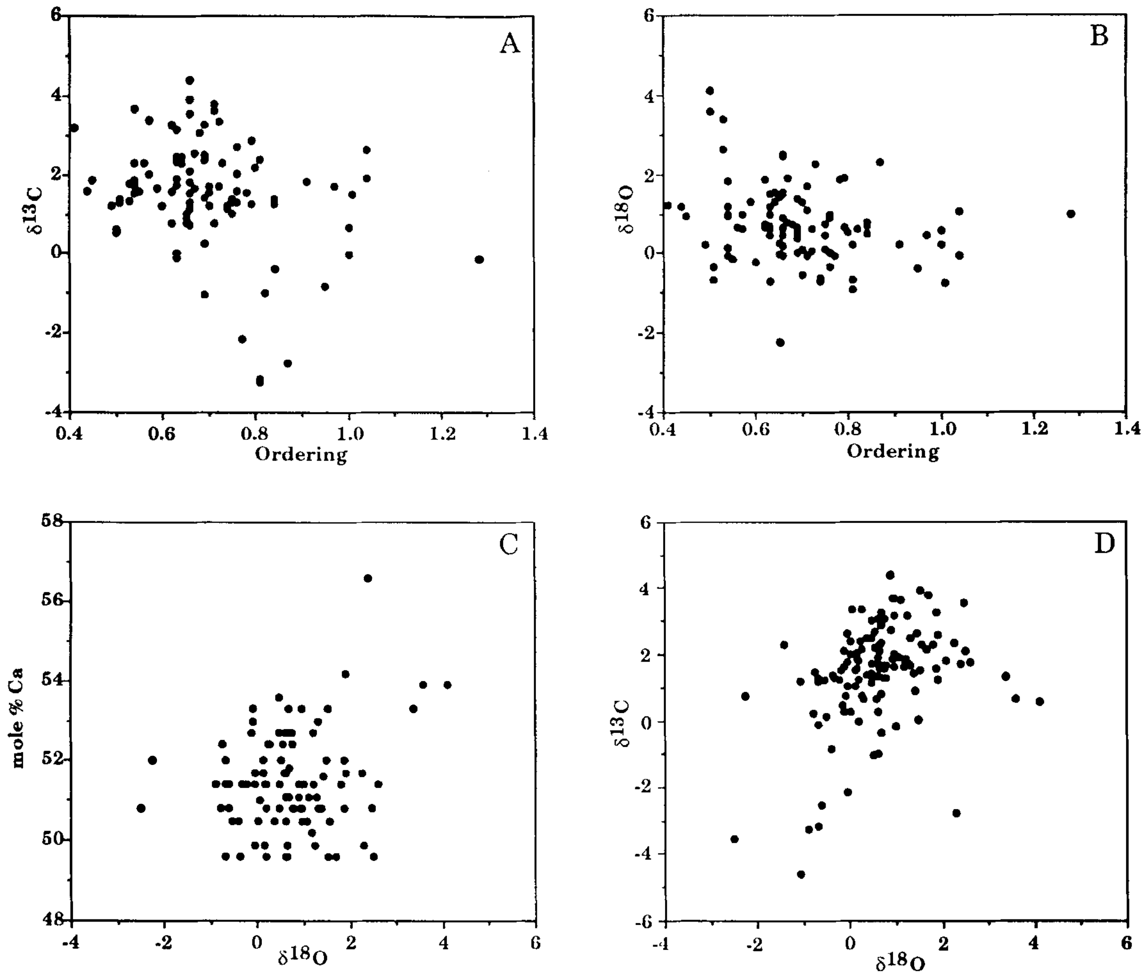

Fig. 6. Bivariant plots of data from the dolomite samples display considerable scatter, and thus very low *r* values were computed for these distributions. Prediction of the value of one variable based on the value of another variable is therefore poor. Nevertheless, statistically significant linear regression trends exist between these pairs of variables (Koch & Link, 1971, Table A. 1). The trends display lower $\delta^{13}C$ and $\delta^{18}O$ values with a higher degree of ordering (A, B), more nearly stoichiometric composition with lower $\delta^{18}O$ values (C), and lower $\delta^{13}C$ values associated with lower $\delta^{18}O$ values (D). Plots (A), (B), (C), (D) display the data for 97, 97, 101 and 122 samples, respectively; a complete listing for each individual sample plotted is listed in Table 2.

addition, the stable isotopic values of the low-magnesian calcitic facies support this interpretation of diagenesis in a meteoric or mixed meteoric and marine water environment (Table 3). The mean $\delta^{18}O$ value of the dolomite is approximately in agreement with dolomite that has formed in contact with waters of the same $\delta^{18}O$ value as the low magnesian calcitic deposits. Thus, the stratigraphic relationships, comparison of the $\delta^{18}O$ values between the dolomitic, aragonitic and calcitic deposits from Al Jubayl, and comparison of the $\delta^{18}O$ values of the Al Jubayl with the Abu Dhabi dolomite indicate that it is highly likely that the Al Jubayl dolomitic strata, subsequent to dolomitization, have been affected by interaction with meteoric or mixed meteoric and marine waters.

The Pleistocene dolomite from the shallow subsurface offshore of Al Jubayl displays interesting differences with those from the modern Abu Dhabi

Table 3. Comparative $\delta^{13}C$ and $\delta^{18}O$ values for whole rock analyses of samples from the aragonitic facies, low magnesian calcitic facies and the dolomitic facies.

	$\delta^{13}C$ (‰, PDB)			$\delta^{18}O$ (‰, PDB)		
Facies	Mean	Range	SD	Mean	Range	SD
Aragonitic (25 analyses)	3·31	4·39 to 2·38	0·60	0·04	0·61 to −1·06	0·31
Low-Mg calcitic (53 analyses)	2·00	3·07 to 0·71	0·56	−2·16	0·33 to −4·32	1·03
Dolomitic (122 analyses)	1·42	4·41 to −4·58	1·54	0·61	4·11 to −2·50	1·04

The samples from the low-magnesian calcitic and dolomitic facies were composed of 100% low-magnesian calcite and dolomite, respectively. The samples from the aragonitic facies are representative of the primary sediment and contain minor amounts of high-magnesian calcite.

Table 4. Comparison of crystal chemistry data for modern dolomite samples analysed by McKenzie (1981) from the Abu Dhabi sabkha and the Pleistocene dolomite analysed during the course of this study.

	Ca content (mol%)	Ordering	$\delta^{13}C$ (‰)	$\delta^{18}O$ (‰)
Abu Dhabi	53·5 (17)	0·36 (17)	2·86 (16)	2·91 (16)
Al Jubayl	51·4 (101)	0·70 (97)	1·42 (122)	0·61 (122)

McKenzie (1981) performed dolomite digestion at 25°C, whereas ours was at 50°C. Our laboratory replicate runs indicate had the dolomite been analysed at 25°C the $\delta^{18}O$ values would have been approximately 0·95‰ higher than those reported.

sabkha (McKenzie, 1981; Table 4). These differences are particularly significant in that the sedimentological evidence indicates that the two accumulations formed under similar conditions. The Pleistocene Al Jubayl dolomite is more nearly ideal stoichiometrically, has a better degree of ordering, and lower $\delta^{13}C$ and $\delta^{18}O$ values than the modern Abu Dhabi dolomite. McKenzie (1981) recognized that the Abu Dhabi Holocene dolomite had undergone diagenetic alteration after the initial dolomitization and referred to this process as an 'ageing' of the dolomite crystals. Carballo *et al.* (1987) also noted, in their investigation of modern dolomite from the Florida Keys, that the older dolomite was less calcium-rich (more nearly ideal stoichiometrically) and better ordered than the younger dolomite. Similar, Holocene dolomite from Ambergis Cay, Belize, displays better ordering with increasing depth (age), but no increase in stoichiometry with depth (Gregg *et al.*, 1992). Ancient dolomite, in general, displays a considerably better degree of ordering, more nearly ideal stoichiometry, and much lower $\delta^{13}C$ and $\delta^{18}O$ values than modern and Pleistocene dolomite (Land, 1980, 1985, 1989; Lumsden & Chimahusky, 1980; Sperber *et al.*, 1984; Smith & Dorobek, 1991). It is, in general, widely accepted that most ancient dolomite has acquired its present attributes (e.g. stoichiometry, trace element composition) due to recrystallization or diagenetic alteration of the original dolomite, either by an iterative process (Land, 1980, 1985, 1989; Tucker & Wright, 1990; Sibley, 1991) or a single step (Sperber *et al.*, 1984). That is, after initial formation of the dolomite, the crystals undergo diagenetic alteration. The covariant trends displayed by the stoichiometry, degree of ordering and stable isotopic values of the Al Jubayl dolomite (Fig. 6) can be interpreted to represent different initial compositions of the dolomite or simultaneous changes in the variables due to diagenesis, changes which resulted in dolomite more similar to that found in the ancient rock record. The latter is interpreted to be correct based on the sedimentology of these deposits as well as the results of other reported studies. Thus, it appears reasonable to assume that the Pleistocene dolomite from Al Jubayl was, at its origin, similar in composition to the modern dolomite of Abu Dhabi and has since undergone diagenetic changes. These changes have given it properties between those of the modern Abu Dhabi dolomite and those sabkha-originated dolomites common in the ancient rock record.

CONCLUSIONS

Pleistocene dolomite from the shallow subsurface offshore of Al Jubayl, Saudi Arabia, formed in a sabkha or in the shallow subsurface of sabkha-related environments. The deposits represent a Quaternary example of a relatively thick dolomite accumulation that formed within these intimately associated environments in which dolomitization occurred in the near surface realm prior to any significant burial.

The Pleistocene dolomite displays a higher degree of ordering, more nearly ideal stoichiometry, and lower $\delta^{13}C$ and $\delta^{18}O$ values than analogous modern sabkha dolomite. This dolomite, subsequent to its initial dolomitization, has been subjected to flushing by water with lower $\delta^{18}O$ values than marine water. These waters must have been either meteoric or mixed meteoric and marine in composition. This has contributed to the diagenetic alteration of the dolomite which has resulted in it displaying attributes between that of modern sabkha dolomite and that found in the ancient rock record.

ACKNOWLEDGMENTS

We gratefully acknowledge the financial assistance of NSF (EAR 8706174) and the Donors of The Petroleum Research Fund administered by the American Chemical Society (PRF 19684-AC2) for the support of this research. We would also like to acknowledge the analytical work of Nancy Utech and Sean Fitzmaurice as well as the contributions of the reviewers, Lynton Land and John Humphrey.

REFERENCES

AL-GHADBAN, A.N. (1990) Holocene sediments in a shallow bay, southern coast of Kuwait, Arabian Gulf. *Mar. Geol.*, **92,** 237–254.

BUTLER, G.P. (1969) Modern evaporite deposition and geochemistry of co-existing brines, the sabkha, Trucial Coast, Arabian Gulf. *J. sedim. Petrol.*, **39,** 70–89.

CARBALLO, J.D., LAND, L.S. & MISER, D.E. (1987) Holocene dolomitization of supratidal sediments by active tidal pumping, Sugarloaf Key Florida. *J. sedim. Petrol.*, **57,** 153–165.

CHAFETZ, H.S., MCINTOSH, A.G. & RUSH, P.F. (1988) Freshwater phreatic diagenesis in the marine realm of recent Arabian Gulf carbonates. *J. sedim. Petrol.*, **58,** 433–440.

CLARKE, M.W.H. & KEIJ, A. J. (1973) Organisms as producers of carbonate sediment and indicators of environment in the southern Persian Gulf: In: *The Persian Gulf* (Ed. by B. H. Purser), pp. 33–56. Springer-Verlag, New York.

CRAIG, H. (1953) The geochemistry of the stable carbon isotopes. *Geochim. Cosmochim. Acta*, **3,** 53–92.

ELLIS, J.P. & MILLIMAN, J.D. (1985) Calcium carbonate suspended in Arabian Gulf and Red Sea waters: biogenic and detrital, not "chemogenic". *J. sedim. Petrol.*, **55,** 805–808.

EMERY, K.O. (1956) Sediments and water of the Persian Gulf. *Bull. Am. Ass. petrol. Geol.*, **40,** 2354–2383.

FUCHTBAUER, H. (Ed.) (1969) Lithification of carbonate sediments, 1. (special issue). *Sedimentology*, **12,** 1–160.

GOLDSMITH, J.R. & GRAF, D.L. (1958) Structural and compositional variations in some natural dolomites. *J. Geol.*, **66,** 678–693.

GOLDSMITH, J.R., GRAF, D.L. & HEARD, H.C. (1961) Lattice constants of the calcium-magnesium carbonates. *Am. Miner.*, **46,** 453–457.

GREGG, J.M., HOWARD, S.A. & MAZZULLO, S.J. (1992) Early diagenetic recrystallization of Holocene (<3000 years old) peritidal dolomites, Ambergris Cay, Belize. *Sedimentology*, **39,** 143–160.

HOUBOULT, J.J.H.C. (1957) *Surface sediments of the Persian Gulf near the Qatar Peninsula.* Dissertation, University of Utrecht.

ILLING, L.V., WELLS, A.J. & TAYLOR, J.C.M. (1965) Penecontemporary dolomite in the Persian Gulf: In: *Dolomitization and Limestone Diagenesis* (Ed. by L. C. Pray & R. C. Murray), *Spec. Publ. Soc. econ. Paleont. Miner.*, **13,** 89–111.

KENDALL, C.G. ST. C. & SKIPWITH, P.A. (1969a) Holocene shallow-water carbonate and evaporite sediments of Khor al Baxam, Abu Dhabi, Southwest Persian Gulf. *Bull. Am. Ass. petrol. Geol.*, **53,** 841–869.

KENDALL, C.G. ST. C. & SKIPWITH, P.A. (1969b) Geomorphology of a recent shallow water carbonate province; Khor al Bazam, southwest Persian Gulf. *Bull. geol. Soc. Am.*, **80,** 865–892.

KHALAF, F., AL-BAKRI, D. & AL-GHADBAN, A. (1984) Sedimentological characteristics of the surficial sediment of the Kuwaiti marine environment, northern Arabian Gulf. *Sedimentology*, **31,** 531–545.

KHALAF, F., MILLIMAN, J.D. & DRUFFEL, E.M. (1987) Submarine limestones in the nearshore environment off Kuwait, northern Arabian Gulf. *Sedimentology*, **34,** 67–75.

KOCH, G.S., JR & LINK, R.F. (1971) *Statistical Analysis of Geological Data*, Vol. 2. John Wiley & Sons, New York.

LAND L.S. (1980) The isotopic and trace element geochemistry of dolomite: the state of the art. In: *Concepts and Models of Dolomitization* (Ed. by D. H. Zenger, J. B. Dunham & R. L. Ethington), *Spec. Publ. Soc. econ. Paleont. Miner.*, **28,** 87–110.

LAND, L.S. (1985) The origin of massive dolomite. *J. geol. Ed.*, **33,** 112–125.

LAND, L.S. (1986) Environments of limestone and dolomite diagenesis: some geochemical considerations. In: *Carbonate Depositional Environments, Modern and Ancient: Part 5: Diagenesis 1* (Ed. by J. E. Warme & K. W. Stanley), *Colo. Sch. Mines Quart.*, **81,** 26–41.

LAND, L.S. (1989) The carbon and oxygen isotopic chemistry of surficial Holocene shallow marine carbonate sediment and Quaternary limestone and dolomite. In: *Handbook of Environmental Isotope Geochemistry* (Ed. by P. Fritz & J. Ch. Fontes), 3, pp. 191–217. Elsevier, Amsterdam.

LUMSDEN, D.N. & CHIMAHUSKY, J.S. (1980) Relationship between dolomite nonstoichiometry and carbonate facies parameters. In: *Concepts and Models of Dolomitization* (Ed. by D. H. Zenger, J. B. Dunham & R. L. Ethington), *Spec. Publ. Soc. econ. Paleont. Miner.*, **28,** 123–137.

MCCREA, J.M. (1950) On the isotopic chemistry of carbonates and a paleotemperature scale. *J. Chem. Phys.*, **18,** 849–857.

MCINTOSH, A.G. (1983) *The depositional environments and diagenesis of sediments from the Arabian Gulf.* MS thesis, University of Houston, Texas.

MCKENZIE, J.A. (1981) Holocene dolomitization of calcium carbonate sediments from the coastal sabkhas of Abu Dhabi, U.A.E.: a stable isotope study. *J. Geol.*, **89,** 185–198.

MCKENZIE, J.A., HSU, K.J. & SCHNEIDER, J.F. (1980) Movement of subsurface waters under the sabkha, Abu Dhabi, UAE, and its relation to evaporative dolomite genesis. In: *Concepts and Models of Dolomitization* (Ed. by D. H. Zenger, J. B. Dunham & R. L. Ethington), *Spec. Publ. Soc. econ. Paleont. Miner.*, **28,** 11–30.

MACHEL, H.-G. & MOUNTJOY, E.W. (1986) Chemistry and environments of dolomitization—A reappraisal. *Earth-Sci. Rev.* **23,** 175–222.

PATTERSON, R.J. & KINSMAN, D.J.J. (1982) Formation of diagenetic dolomite in coastal sabkha along Arabian (Persian) Gulf. *Bull. Am. Ass. petrol. Geol.*, **66,** 28–43.

PICHA, F. (1978) Depositional and diagenetic history of Pleistocene and Holocene oolitic sediments and sabkhas in Kuwait, Persian Gulf. *Sedimentology,* **25,** 427–449.

PIERCE, D. B. (1990) *Petrography and provenance of siliciclastic sands from a carbonate environment—Arabian Gulf, Saudi Arabia.* M.S. thesis, University of Houston, Texas.

PURSER, B.H. (Ed.) (1973a) *The Persian Gulf; Holocene Carbonate Sedimentation and Diagenesis in a Shallow Epicontinental Sea.* Springer-Verlag, New York.

PURSER, B.H. (1973b) Sedimentation around bathymetric highs in the Southern Persian Gulf: In: *The Persian Gulf* (Ed. by B. H. Purser), pp. 157–177. Springer-Verlag, New York.

PURSER, B.H. (1979) Quaternary carbonate sedimentation and diagenesis in the Persian/Arabian Gulf. *Am. Assoc. petrol. Geol. Lec. Notes,* 1–56.

SHARMA, T. & CLAYTON, R.N. (1965) Measurement of O^{18}/O^{16} ratios of total oxygen of carbonates. *Geochim. Cosmochim. Acta,* **29,** 1347–1353.

SIBLEY, D.F. (1991) Dolomite mineralogy and texture in time and space. In: *Dolomieu Conf. on Carbonate Platforms and Dolomitization*, p. 245 (abstract).

SMITH, T.M. & DOROBEK, S.L. (1991) Dolomite recrystallization in the presence of meteoric water: geochemical and petrographic constraints from the Mississippian Mission Canyon Formation, central to southwestern Montana. In: *Dolomieu Conf. on Carbonate Platforms and Dolomitization*, p. 249 (abstract).

SPERBER, C.M., WILKINSON, B.H. & PEACOR, D.R. (1984) Rock composition, dolomite stoichiometry, and rock/water reactions in dolomitic carbonate rocks. *J. Geol.*, **92,** 609–622.

TUCKER, M.E. & WRIGHT, V.P. (1990) *Carbonate Sedimentology*. Blackwell Scientific Publications, Oxford.

WAGNER, C.W. & VAN DER TOGT, C. (1973) Holocene sediment types and their distribution in the southern Persian Gulf. In: *The Persian Gulf* (Ed. by B. H. Purser), pp. 123–156. Springer-Verlag, New York.

WELLS, A.J. & ILLING, L.V. (1964) Present day precipitation of calcium carbonate in the Persian Gulf. In: *Deltaic and Shallow Water Marine Deposits* (Ed. by L. M. J. U. Van Straten), pp. 429–435. Elsevier, Amsterdam.

(Manuscript received 6 April 1993; revision accepted 17 September 1993)